Modeling diffusion around the cathode in a low-temperature carbon dioxide reduction cell

Lucas de Kam

March 2021

Abstract

Through electrochemical reduction, the greenhouse gas CO_2 can be converted into useful chemicals. The first step in such an electrochemical reduction process is the reduction of CO_2 to CO. This can be achieved at room temperature using a so-called low-temperature reduction cell. In this system, CO_2 is dissolved in an aqueous solution that is in contact with a cathode, where the reduction reaction takes place. In this RP project, I modeled the steady-state concentration profile of aqueous CO_2 and related species in the diffusion layer at the cathode. To do this, I derived simplified boundary conditions and solved the relevant system of diffusion equations numerically in Python.

1 Introduction

Due to the widespread use of fossil fuels, anthropogenic CO_2 emissions greatly exceed the earth's natural carbon intake. This has serious consequences for our climate (Gattuso et al., 2015). It is therefore of major importance for our society to close the carbon cycle. Besides drastically reducing CO_2 emissions, we can also increase our intake of CO_2.

The process of electrochemical CO_2 reduction does exactly that: it uses electricity to convert waste CO_2 into useful chemicals. By using excess electricity from intermittent renewable energy sources, the process could be used to tackle two challenges at once: closing the carbon cycle, and energy storage. Although the ultimate goal is to be able to convert CO_2 back into valuable hydrocarbons and alcohols (Kibria et al., 2019; Liu et al., 2017; Weekes et al., 2018), the easiest step is to convert it into CO, which is the focus of this report.

The reduction process can take place at room temperature in a low-temperature reduction cell, where CO_2 is dissolved in an aqueous solution (Figure 1). This is in contrast to e.g. solid oxide electrolyzers, where the reduction occurs at temperatures between 500 and 1000 °C (Küngas, 2020; Weekes et al., 2018). In low-temperature reduction cells, the selectivity towards a certain product depends strongly on the pH (Hori et al., 1989). It is therefore important to understand how the pH behaves near the cathode, where the reduction reaction takes place.

As such, the aim for this RP project was to model the steady-state profiles of aqueous CO_2 concentration and the pH near the cathode in a low-temperature CO_2

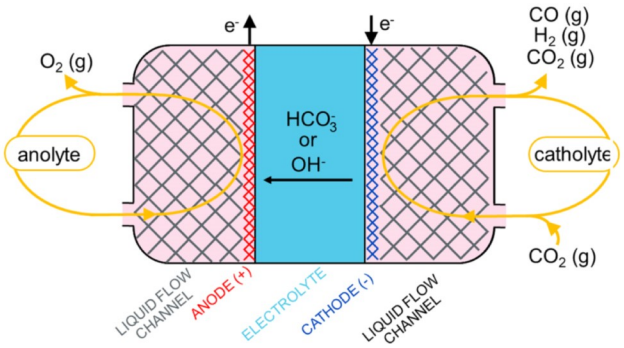

Figure 1: Low-temperature CO_2 reduction flow cell. CO_2 is dissolved in an aqueous solution (the catholyte) which is in contact with the cathode, where the reduction reaction takes place. At the anode, water or OH^- is oxidized to form oxygen. Figure taken from Küngas (2020); licensed under a CC BY-NC-ND license.

reduction cell at various current densities. In addition, I will include concentration profiles of other species in the solution.

In the Theory section, I will introduce the reactions that take place and compute the equilibrium concentration of the species in the solution. I will also formulate the differential equations that are to be solved in order to obtain the concentration profiles. Next, in the Methods section, I explain how I solved these differential equations in Python. I then show the results and discuss them, and I end with some concluding remarks and directions for further development of the model.

2 Theory

In a low-temperature CO_2 reduction cell, formation of CO competes with other reactions, depending on the pH at the cathode (Hori et al., 1989). One example of such a side reaction is the formation of hydrogen through the electrolysis of water (Küngas, 2020). To increase the selectivity towards CO (in other words, to improve the Faradaic efficiency), low-temperature CO_2 reduction cells operate under slightly basic (pH > 7) conditions (Küngas, 2020). In a basic solution, the reduction of CO_2 to CO at the cathode is described as

$$CO_2(aq) + H_2O(l) + 2\,e^- \longrightarrow CO(aq) + 2\,OH^-(aq). \tag{1}$$

To obtain the steady state concentration profiles for the species in the solution near the cathode, we need to know the differential equations that govern the concentrations of the species, and the boundary conditions.

Let us consider a one-dimensional system with the cathode surface at $x = 0$ (Figure 2). It is common to assume that the concentrations only vary from the bulk solution (the catholyte) in a thin layer near the electrode called the diffusion layer, which has thickness L. In this diffusion layer, convective transport is negligible (Gupta et al., 2006). Following Gupta et al. (2006), I will take $L = 100\ \mu$m. Now, the aim

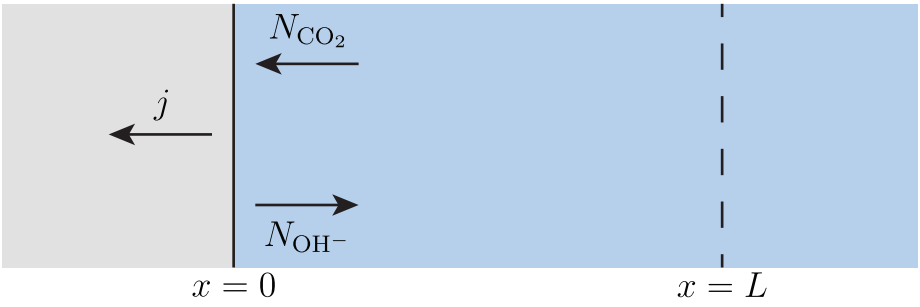

Figure 2: Schematic of the system. The cathode surface is located at $x = 0$, and the diffusion layer is between $x = 0$ and $x = L$. j is the current density, N_{CO_2} the flux of aqueous CO_2 at the cathode surface and N_{OH^-} the hydroxide ion flux at the cathode surface.

is to obtain the steady-state concentration profile for $0 \leq x \leq L$, with boundary conditions at $x = 0$ related to the CO_2 reduction rate at the cathode, and boundary conditions at $x = L$ given by the concentrations in the bulk solution.

I will first calculate the bulk concentration of aqueous CO_2, and after introducing the reactions that occur in the solution, I will calculate the bulk concentrations of the other relevant species. Next, I calculate the boundary conditions at the cathode surface using the stoichiometry of the reduction reaction. I finally introduce the differential equations that govern the concentrations of each species.

2.1 Bulk concentration of aqueous carbon dioxide

In order for CO_2 to reach the cathode, it must first be dissolved in the catholyte. The dissolution of gaseous CO_2 in water is described by the following chemical equilibrium:

$$CO_2(g) \rightleftharpoons CO_2(aq). \tag{2}$$

The equilibrium constant for this reaction is known as the Henry's law constant H, which is the ratio of the concentration of aqueous CO_2 to the partial pressure of gaseous CO_2. I will denote concentrations using square brackets, so that the concentration of $CO_2(aq)$ is written as $[CO_2(aq)]$. Writing the partial pressure of CO_2 in the gas that is in contact with the solution as P_{CO_2}, Henry's law can be written as

$$H = \frac{[CO_2(aq)]}{P_{CO_2}}. \tag{3}$$

At 298 K, $H = 3.4 \times 10^{-4} \frac{\text{mol}}{\text{m}^3\text{Pa}}$ (Sander, 2015). For a solution exposed to $CO_2(g)$ with a partial pressure of 1 atm, the concentration is then

$$[CO_2(aq)] = HP_{CO_2} \approx 34.45 \,\text{mol}\,\text{m}^{-3}. \tag{4}$$

This value corresponds to data from Wikipedia (n.d.) and Küngas (2020). I will assume the ideal case in which the catholyte is continuously saturated to this concentration of aqueous CO_2. Assuming also that all species formed in reactions at the

cathode and in the solution are aqueous, I will omit the (aq) notation for aqueous species from now on.

2.2 Reactions in the catholyte

An aqueous solution of CO_2 by itself is slightly acidic (Butler, 1991, Chapter 2). To raise the pH and increase specificity towards the formation of CO, it is necessary to add a base such as a bicarbonate buffer (Gupta et al., 2006). To simplify the calculations, I will assume here that a strong base, NaOH, is added until the amount of added base equals the total amount of carbon species in the solution (as described by Butler (1991, Chapter 2)).

In a basic solution with CO_2, the following two reactions occur (Knuutila et al., 2010; Gupta et al., 2006). First, CO_2 can react with OH^- to form a bicarbonate anion:

$$CO_2 + OH^- \rightleftharpoons HCO_3^-, \tag{5}$$

with equilibrium constant $K_1 = 4.44 \times 10^4\ \mathrm{m^3\ mol^{-1}}$ (Gupta et al., 2006). Note that this reaction is essentially the dissociation of H_2CO_3,

$$CO_2 + H_2O(l) \rightleftharpoons HCO_3^- + H^+,$$

but written for a basic solution. The second reaction is the formation of carbonate ions from bicarbonate ions:

$$HCO_3^- + OH^- \rightleftharpoons CO_3^{2-} + H_2O(l), \tag{6}$$

with equilibrium constant $K_2 = 4.66\ \mathrm{m^3\ mol^{-1}}$ (Gupta et al., 2006).

2.3 Bulk concentrations and bulk pH

So far, we only know the concentration of CO_2 in the bulk solution (eq. 4). To determine the equilibrium concentrations in the bulk solution for the other relevant species, namely OH^-, HCO_3^- and CO_3^{2-}, we need three equations. The chemical equilibria (5) and (6) give us the first two:

$$K_1 = \frac{[HCO_3^-]}{[CO_2][OH^-]} \tag{7}$$

and

$$K_2 = \frac{[CO_3^{2-}]}{[HCO_3^-][OH^-]}. \tag{8}$$

We can find a third equation by considering that the sum of all charges in the solution should be zero. The charge balance reads

$$[H^+] + [Na^+] = [HCO_3^-] + 2[CO_3^{2-}] + [OH^-]. \tag{9}$$

Now, because we assumed that the amount of NaOH added equals the amount of dissolved carbon species,

$$[Na^+] = [CO_2] + [HCO_3^-] + [CO_3^{2-}].$$

Plugging this expression into equation (9) and neglecting the small concentrations of H^+ and OH^-, we obtain that

$$[CO_2] \approx [CO_3^{2-}], \tag{10}$$

and because $[CO_2]$ is known (eq. 4), this gives us an expression for the carbonate ion concentration. Using equations (7) and (8) we can rewrite $[CO_3^{2-}]$ such that the equation becomes

$$[CO_2] = [CO_2][OH^-]^2 K_1 K_2,$$

and this can be rearranged to yield

$$[OH^-] = \frac{1}{\sqrt{K_1 K_2}}. \tag{11}$$

Plugging this back into equation (7) gives us $[HCO_3^-]$. In summary, the equilibrium concentrations for the assumptions made here can be calculated as follows:

$$[CO_2] = HP_{CO_2} \tag{12}$$

$$[OH^-] = \frac{1}{\sqrt{K_1 K_2}} \tag{13}$$

$$[HCO_3^-] = H\sqrt{\frac{K_1}{K_2}} P_{CO_2} \tag{14}$$

$$[CO_3^{2-}] = HP_{CO_2}. \tag{15}$$

Since $[H^+] = K_w/[OH^-]$ with $K_w = 10^{-14.0}$ the equilibrium constant for the ionization of water (Butler, 1991, Chapter 1), we can calculate the pH of the bulk solution as

$$\mathrm{pH} = -\log [H^+](\mathrm{M}) = 14 - \frac{1}{2}\log(K_1 K_2) \approx 8.34. \tag{16}$$

In the above formula, $[H^+](\mathrm{M})$ means that $[H^+]$ must be written in units of $\mathrm{M} = \mathrm{mol\,L^{-1}}$.

Making assumptions on the amount of base added allowed for analytic solutions. For other amounts of base added, equations (7), (8), and (9) could be solved numerically. It is then also possible to do a numerical calculation for different bases, such as potassium bicarbonate, given that the equations are adapted appropriately.

2.4 Cathode boundary conditions

At the cathode, CO_2 is reduced to CO, as described by reaction (1). For simplicity I assume that all current through the electrode is used only for this reaction – in other words, I assume that the reduction to CO has a Faradaic efficiency of 100%.

The stoichiometry of the reaction allows us to relate the flux of CO_2 towards the electrode surface to the current density in the electrode. For one mole of CO_2 coming in (in the negative x-direction), half a mole of electrons is used up, so the molar flux at the electrode surface $N_{CO_2}|_{x=0}$ is given by

$$N_{CO_2}\Big|_{x=0} = \frac{1}{2}\frac{j}{F},$$

where F is Faraday's constant. Note that electrons flow out of the cathode (in the positive x-direction), so the current is directed towards negative x, and therefore j is negative. For a dilute solution (Bird et al., 2002, Chapter 18.4),

$$N_{CO_2} = -D_{CO_2} \frac{\partial [CO_2]}{\partial x},$$

with D_{CO_2} the diffusion coefficient for CO_2, the value of which is listed in Table 1. Combining the two expressions, we obtain the boundary condition

$$\left. \frac{\partial [CO_2]}{\partial x} \right|_{x=0} = -\frac{1}{2D_{CO_2}} \frac{j}{F}. \tag{17}$$

Since OH^- is produced at the cathode surface, we can derive the boundary condition for $[OH^-]$ in a similar way:

$$\left. \frac{\partial [OH^-]}{\partial x} \right|_{x=0} = \frac{1}{D_{OH^-}} \frac{j}{F}. \tag{18}$$

The other two species, HCO_3^- and CO_3^{2-}, do not react at the cathode, and therefore I will assume that their flux at $x = 0$ is zero, i.e.

$$\left. \frac{\partial [HCO_3^-]}{\partial x} \right|_{x=0} = \left. \frac{\partial [CO_3^{2-}]}{\partial x} \right|_{x=0} = 0. \tag{19}$$

2.5 Diffusion equations

To find the concentration profiles for the different species we can solve the diffusion equations based on the respective reactions (see for instance Bird et al. (2002), Chapter 19.1). Because of the reactions (5) and (6), these equations are coupled:

$$\frac{\partial [CO_2]}{\partial t} = D_{CO_2} \frac{\partial^2 [CO_2]}{\partial x^2} - k_{1f}[CO_2][OH^-] + k_{1r}[HCO_3^-] \tag{20}$$

$$\begin{aligned} \frac{\partial [OH^-]}{\partial t} = {} & D_{OH^-} \frac{\partial^2 [OH^-]}{\partial x^2} - k_{1f}[CO_2][OH^-] + k_{1r}[HCO_3^-] \\ & - k_{2f}[HCO_3^-][OH^-] + k_{2r}[CO_3^{2-}] \end{aligned} \tag{21}$$

$$\begin{aligned} \frac{\partial [HCO_3^-]}{\partial t} = {} & D_{HCO_3^-} \frac{\partial^2 [HCO_3^-]}{\partial x^2} + k_{1f}[CO_2][OH^-] - k_{1r}[HCO_3^-] \\ & - k_{2f}[HCO_3^-][OH^-] + k_{2r}[CO_3^{2-}] \end{aligned} \tag{22}$$

$$\frac{\partial [CO_3^{2-}]}{\partial t} = D_{CO_3^{2-}} \frac{\partial^2 [CO_3^{2-}]}{\partial x^2} + k_{2f}[HCO_3^-][OH^-] - k_{2r}[CO_3^{2-}]. \tag{23}$$

Here, D_i is the diffusion coefficient for species i; k_{1f} and k_{1r} are the forward and reverse reaction rate constants for reaction (5); and finally, k_{2f} and k_{2r} are the forward and reverse reaction rate constants for reaction (6). The values for the diffusion coefficients are listed in Table 1 and the rate constants in Table 2.

Solving for the steady-state concentration profiles means that the time derivatives are set to zero. In doing so, the problem is reduced to a system of coupled ordinary differential equations.

D_{CO_2} ($m^2\ s^{-1}$)	D_{OH^-} ($m^2\ s^{-1}$)	$D_{HCO_3^-}$ ($m^2\ s^{-1}$)	$D_{CO_3^{2-}}$ ($m^2\ s^{-1}$)
1.91×10^{-9}	5.27×10^{-9}	1.19×10^{-9}	9.23×10^{-10}

Table 1: Diffusion coefficients for different species at infinite dilution in water at 298 K. Data from Lide (2004).

Reaction	Forward rate constant ($m^3\ mol^{-1}\ s^{-1}$)	Reverse rate constant (s^{-1})
5	$k_{1f} = 5.93$	$k_{1r} = 1.34 \times 10^{-4}$
6	$k_{2f} = 1 \times 10^5$ (assumption)	$k_{2r} = 2.15 \times 10^4$

Table 2: Rate constants for the reactions given by the chemical equations (5) and (6) at 298 K. Data (including the assumption for k_{2f}) from Gupta et al. (2006).

3 Methods

As described in the Theory section, the objective is now to solve a system of coupled differential equations as given by equations (20-23) where the time derivatives are zero. This gives

$$-D_{CO_2}\frac{\partial^2[CO_2]}{\partial x^2} = -k_{1f}[CO_2][OH^-] + k_{1r}[HCO_3^-] \tag{24}$$

$$-D_{OH^-}\frac{\partial^2[OH^-]}{\partial x^2} = -k_{1f}[CO_2][OH^-] + k_{1r}[HCO_3^-] - k_{2f}[HCO_3^-][OH^-] + k_{2r}[CO_3^{2-}] \tag{25}$$

$$-D_{HCO_3^-}\frac{\partial^2[HCO_3^-]}{\partial x^2} = k_{1f}[CO_2][OH^-] - k_{1r}[HCO_3^-] - k_{2f}[HCO_3^-][OH^-] + k_{2r}[CO_3^{2-}] \tag{26}$$

$$-D_{CO_3^{2-}}\frac{\partial^2[CO_3^{2-}]}{\partial x^2} = k_{2f}[HCO_3^-][OH^-] - k_{2r}[CO_3^{2-}], \tag{27}$$

with boundary conditions at $x = L \approx 100\ \mu$m given by equations (12-15) and boundary conditions at $x = 0$ given by (17-19). I rewrote the above system to a system of eight coupled first-order ODEs, which I solved in Python using the Scipy function `integrate.solve_bvp` (Virtanen et al., 2020).

The Jupyter notebook with the Python code is available on GitHub: `https://github.com/lucasdekam/co2diffusion`.

4 Results and discussion

Common current densities range between orders of 10^{-3} A cm^{-2} to 10^{-6} A cm^{-2} (Ryu et al., 1972; Gupta et al., 2006). The obtained steady-state concentration profiles for four current densities in this range are shown in Figure 3. A higher current

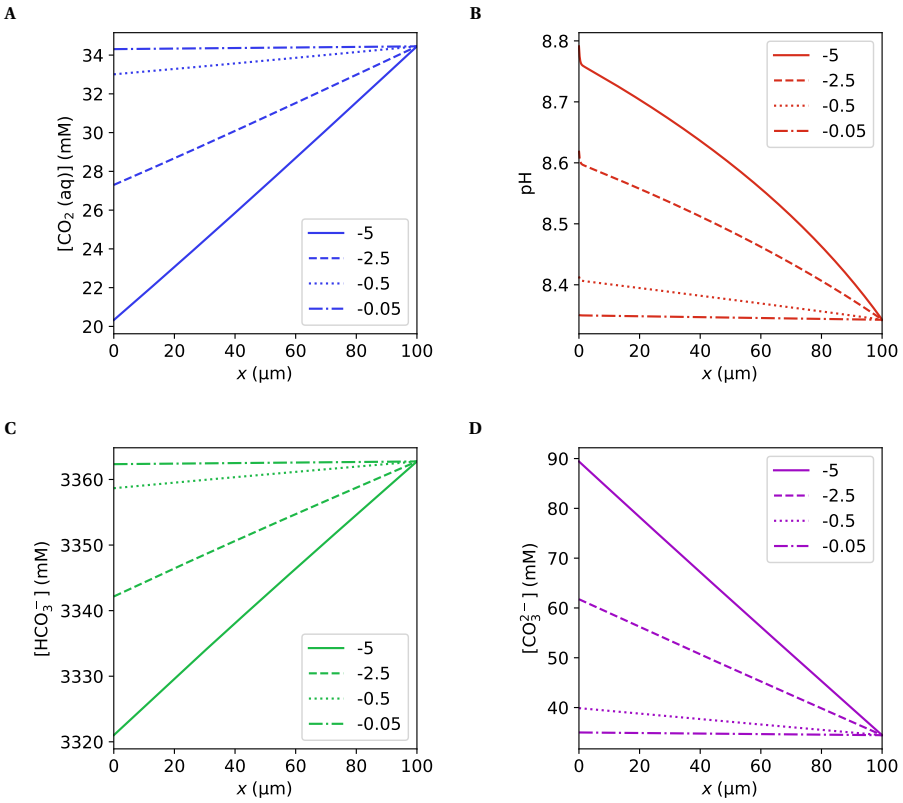

Figure 3: Steady-state concentration profiles at four different current densities j: -5 mA cm^{-2}, -2.5 mA cm^{-2}, -0.5 mA cm^{-2} and -0.05 mA cm^{-2}. The legends indicate the current density in units of mA cm^{-2}. The minus signs are due to the fact that the current runs in the negative x-direction (Figure 2). **A**, **C** and **D** show the concentration profiles for CO_2, HCO_3^- and CO_3^{2-}, respectively. **B** shows the pH profile.

density causes a higher reaction rate and thus a greater flux of CO_2 into the electrode. This can be observed in Figure 3A as a steeper slope of the concentration profile. Besides, the formation of OH^- at the electrode also increases with the current density, which increases the pH near the electrode (Figure 3B). Despite the zero-flux boundary conditions for HCO_3^- and CO_3^{2-}, the slope is rather steep near $x = 0$ in these concentration profiles for higher current densities (Figures 3C, 3D).

The concentration profiles are similar to results from more extensive models by Ager (2020) and Gupta et al. (2006), who solved for the bulk concentrations numerically for the case where a bicarbonate buffer solution is used. Although this different boundary condition causes the concentration values for HCO_3^- and CO_3^{2-} and the pH to be different from mine, the general behavior of the concentrations is still the same. Ager and Gupta et al. use the same bulk concentration for CO_2; therefore the steady-state CO_2 concentration profiles they obtained are nearly identical to Figure

3A. The small difference in the concentration at the cathode surface could be caused by their incorporation of other reactions at the cathode.

5 Conclusion

In this report I presented the steady-state concentration profiles of relevant species near the cathode in a low-temperature CO_2 reduction process. The concentration profiles were obtained by solving a system of diffusion equations numerically in Python. The bulk concentration boundary conditions were derived using simplifying assumptions, and the flux boundary conditions at the electrode were derived using the stoichiometry of the reduction reaction. The results show behavior that is qualitatively similar to results from more extensive models in literature. As such, the presented model gives a qualitative understanding of how the concentrations and the pH behave around the cathode.

To make this model more realistic and useful, the main priority of future work should be to calculate the bulk concentrations of relevant species numerically, as implemented by Ager (2020). This would make it possible to do calculations for different types of catholytes. Side reactions at the cathode may also be considered, such as the formation of hydrogen (Küngas, 2020). Finally, the model may be extended to allow for time-dependent solutions. This would require using a more advanced numerical solver such as FEniCS by Alnaes et al. (2015), which was also used by Ager (2020).

References

Ager, J. W. (2020). Cathode surface concentrations for the electrochemical reduction of carbon dioxide in bicarbonate buffer solutions.
URL: `github.com/joelager/CO2-electrochemical-reaction-diffusion`

Alnaes, M. S., Blechta, J., Hake, J., Johansson, A., Kehlet, B., Logg, A., Richardson, C., Ring, J., Rognes, M. E. and Wells, G. N. (2015). The FEniCS project version 1.5, *Archive of Numerical Software* **3**. DOI: 10.11588/ans.2015.100.20553.

Bird, R. B., Stewart, W. E. and Lightfoot, E. N. (2002). *Transport Phenomena (2nd ed.)*, John Wiley and Sons, Inc.

Butler, J. (1991). *Carbon Dioxide Equilibria and their Applications (1st ed.)*, CRC Press.

Gattuso, J.-P., Magnan, A., Billé, R., Cheung, W. W., Howes, E. L., Joos, F., Allemand, D., Bopp, L., Cooley, S. R., Eakin, C. M. et al. (2015). Contrasting futures for ocean and society from different anthropogenic CO2 emissions scenarios, *Science* **349**(6243).

Gupta, N., Gattrell, M. and MacDougall, B. (2006). Calculation for the cathode surface concentrations in the electrochemical reduction of CO2 in KHCO3 solutions, *Journal of applied electrochemistry* **36**(2): 161–172.

Hori, Y., Murata, A. and Takahashi, R. (1989). Formation of hydrocarbons in the electrochemical reduction of carbon dioxide at a copper electrode in aqueous solution, *Journal of the Chemical Society, Faraday Transactions 1: Physical Chemistry in Condensed Phases* **85**(8): 2309–2326.

Kibria, M. G., Edwards, J. P., Gabardo, C. M., Dinh, C.-T., Seifitokaldani, A., Sinton, D. and Sargent, E. H. (2019). Electrochemical CO2 reduction into chemical feedstocks: from mechanistic electrocatalysis models to system design, *Advanced Materials* **31**(31): 1807166.

Knuutila, H., Juliussen, O. and Svendsen, H. F. (2010). Kinetics of the reaction of carbon dioxide with aqueous sodium and potassium carbonate solutions, *Chemical Engineering Science* **65**(23): 6077–6088.

Küngas, R. (2020). Electrochemical CO2 reduction for CO production: comparison of low-and high-temperature electrolysis technologies, *Journal of The Electrochemical Society* **167**(4): 044508.

Lide, D. R. (2004). *CRC handbook of chemistry and physics*, Vol. 85, CRC press.

Liu, X., Xiao, J., Peng, H., Hong, X., Chan, K. and Nørskov, J. K. (2017). Understanding trends in electrochemical carbon dioxide reduction rates, *Nature communications* **8**(1): 1–7.

Ryu, J., Andersen, T. and Eyring, H. (1972). Electrode reduction kinetics of carbon dioxide in aqueous solution, *The Journal of Physical Chemistry* **76**(22): 3278–3286.

Sander, R. (2015). Compilation of Henry's law constants (version 4.0) for water as solvent, *Atmospheric Chemistry and Physics* **15**(8): 4399–4981.

Virtanen, P., Gommers, R., Oliphant, T. E., Haberland, M., Reddy, T., Cournapeau, D., Burovski, E., Peterson, P., Weckesser, W., Bright, J., van der Walt, S. J., Brett, M., Wilson, J., Millman, K. J., Mayorov, N., Nelson, A. R. J., Jones, E., Kern, R., Larson, E., Carey, C. J., Polat, İ., Feng, Y., Moore, E. W., VanderPlas, J., Laxalde, D., Perktold, J., Cimrman, R., Henriksen, I., Quintero, E. A., Harris, C. R., Archibald, A. M., Ribeiro, A. H., Pedregosa, F., van Mulbregt, P. and SciPy 1.0 Contributors (2020). SciPy 1.0: Fundamental Algorithms for Scientific Computing in Python, *Nature Methods* **17**: 261–272. DOI: 10.1038/s41592-019-0686-2.

Weekes, D. M., Salvatore, D. A., Reyes, A., Huang, A. and Berlinguette, C. P. (2018). Electrolytic CO2 reduction in a flow cell, *Accounts of chemical research* **51**(4): 910–918.

Wikipedia (n.d.). Carbon dioxide (data page).
URL: https://en.wikipedia.org/wiki/Carbon_dioxide_(data_page)